Dispersion of nonlinearity and modulation instability in subwavelength semiconductor waveguides

A.V. Gorbach, X. Zhao, and D.V. Skryabin*

Centre for Photonics and Photonic Materials, Department of Physics, University of Bath, Bath BA2 7AY, UK

**Corresponding author: d.v.skryabin@bath.ac.uk*

Abstract: Tight confinement of light in subwavelength waveguides induces substantial dispersion of their nonlinear response. We demonstrate that this dispersion of nonlinearity can lead to the modulational instability in the regime of normal group velocity dispersion through the mechanism independent from higher order dispersions of linear waves. A simple phenomenological model describing this effect is the nonlinear Schrödinger equation with the intensity dependent group velocity dispersion.

OCIS codes: 190.4380 (Nonlinear optics, four-wave mixing); 190.4970 (Parametric oscillators and amplifiers); 130.4310 (Integrated optics, nonlinear).

References and links

1. M. Kolesik, E. M. Wright, J. V. Moloney, "Simulation of femtosecond pulse propagation in sub-micron diameter tapered fibers," Appl. Phys. B **79**, 293-300 (2004).
2. A. V. Gorbach and D. V. Skryabin, "Spatial solitons in periodic nanostructures," Phys. Rev. A **79**, 053812 (2009).
3. S. Afshar V., T. M. Monro, " A full vectorial model for pulse propagation in emerging waveguides with subwavelength structures part I: Kerr nonlinearity," Opt. Express **17**, 2298-2318 (2009).
4. T. X. Tran and F. Biancalana, "An accurate envelope equation for light propagation in photonic nanowires: new nonlinear effects," Opt. Express **17**, 17934-17949 (2009).
5. N. C. Panoiu, X. P. Liu, R. M. Osgood, Jr., "Self-steepening of ultrashort pulses in silicon photonic nanowires," Opt. Lett. **34**, 947-949 (2009).
6. A. V. Gorbach, W. Ding, O. K. Staines, C. E. de Nobriga, G. D. Hobbs, W. J. Wadsworth, J. C. Knight, D. V. Skryabin, A. Samarelli, M. Sorel, and R. M. De La Rue, "Spatiotemporal nonlinear optics in arrays of subwavelength waveguides," Phys. Rev. A. **82**, 041802 (2010).
7. Q. Lin, J. Zhang, P. M. Fauchet, G. P. Agrawal, "Ultrabroadband parametric generation and wavelength conversion in silicon waveguides," Opt. Express **14**, 4786-4799 (2006).
8. R. M. Osgood, Jr., N. C. Panoiu, J. I. Dadap, X. Liu, X. Chen, I.-W. Hsieh, E. Dulkeith, W. M. Green, and Y. A. Vlasov, "Engineering nonlinearities in nanoscale optical systems: physics and applications in dispersion-engineered silicon nanophotonic wires," Adv. Opt. Photon. **1**, 162-235 (2009).
9. M. Galili, J. Xu, H. C. Mulvad, L. K. Oxenløwe, A. T. Clausen, P. Jeppesen, B. Luther-Davies, S. Madden, A. Rode, D.-Y. Choi, M. Pelusi, F. Luan, and B. J. Eggleton, "Breakthrough switching speed with an all-optical chalcogenide glass chip: 640 Gbit/s demultiplexing," Opt. Express **17**, 2182-2187 (2009).
10. M. A. Foster, A. C. Turner, J. E. Sharping, B. S. Schmidt, M. Lipson, A. L. Gaeta "Broad-band optical parametric gain on a silicon photonic chip," Nature **441**, 960-963 (2006).
11. S. B. Cavalcanti, J. C. Cressoni, H. R. da Cruz, and A. S. Gouveia-Neto, "Modulation instability in the region of minimum group-velocity dispersion of single-mode optical fibers via an extended nonlinear Schrödinger equation," Phys. Rev. A **43**, 6162–6165 (1991).
12. F. Biancalana, D. V. Skryabin, and P. St. J. Russell, "Four-wave mixing instabilities in photonic-crystal and tapered fibers," Phys. Rev. E **68**, 046603 (2003).
13. G. Van Simaeys, Ph. Emplit, and M. Haelterman, "Experimental Demonstration of the Fermi-Pasta-Ulam Recurrence in a Modulationally Unstable Optical Wave," Phys. Rev. Lett. **87**, 033902 (2001).

14. C. Koos, P. Vorreau, T. Vallaitis, P. Dumon, W. Bogaerts, R. Baets, B. Esembeson, I. Biaggio, T. Michinobu, F. Diederich, W. Freude, and J. Leuthold, "All-optical high-speed signal processing with silicon-organic hybrid slot waveguides," Nature Photonics **3**, 216-219 (2009).
15. M. J. Potasek, "Modulation instability in an extended nonlinear Schrdinger equation," Opt. Lett. 12, 921-923 (1987)
16. Y. Xiang *et al.*, "Modulation instability induced by nonlinear dispersion in nonlinear metamaterials," J. Opt. Soc. Am. B **24**, 3058-3063 (2007).

Theory and modeling of nonlinear light propagation in subwalength structures have attracted significant recent attention, see, e.g., [1, 2, 3, 4, 5, 6, 7, 8] and references therein, following remarkable progress with fabrication and a stimulus coming from the need of small footprint photonic devices for information processing applications. Modulational instability (MI) is a well known and important for optical demultiplexing and other applications effect, which has been extensively studied in the chip scale geometries, see, e.g., [8, 9, 10]. MI constitutes a process where a constant amplitude pump wave at frequency ω_p is able to create parametric gain for the side-bands at frequencies ω_s (signal) and $\omega_i = 2\omega_p - \omega_s$ (idler).

For the most typical focusing Kerr nonlinearity a well known necessary condition for the MI to exist is determined solely by the dispersion of linear waves. It is expressed as $\delta\beta = 2\beta_p - \beta_s - \beta_i > 0$, where $\beta_{p,s,i} = \beta(\omega_{p,s,i})$ are the propagation constants at the respective frequencies, see, e.g. [12] and references therein. If the waveguide dispersion is dominated by the group velocity dispersion (GVD), $\delta\beta \simeq -\beta_2(\omega_p - \omega_s)^2$, then MI requires that the GVD coefficient at the pump frequency is negative $\beta_2 = \partial^2_\omega \beta(\omega_p) < 0$, i.e. GVD is anomalous. If $|\beta_2(\omega_p)|$ is relatively small or zero, then the dispersion coefficients of other even orders determine presence or absence of MI [11, 12]. This well established picture is based on the assumption that propagation obeys the nonlinear Schrödinger (NLS) equation with a nondispersive nonlinear parameter. So far the most studied dispersive corrections to the nonlinearity have been the self-steepening term, which introduces dependence of group velocity on light intensity, and Raman nonlinearity, see, e.g., [4, 5, 15, 16]. Group velocity term, $\partial_\omega \beta(\omega_p)$, and hence self-steepening, along with other odd order coefficients in the expansion of β make no impact on the conditions required for MI gain [11, 12, 15]. Raman effect and delayed nonlinear responses of other physical origins [4, 15], while able to influence MI, have different (non-parametric) nature. They do not conserve total energy of the participating photons and the spectral range of the Raman gain is determined by the material properties and not by the wavenumber matching conditions. We disregard any non-parametric effects in what follows. Recently it has been demonstrated that the nonlinearity and magnetic permeability in metamaterials make a strong effective dispersion of nonlinearity, impacting MI [16].

Below we demonstrate, that the frequency dependence of the nonlinear coefficients mediating interaction of the pump, signal and idler photons can generate MI gain when the pump frequency is located in the normal GVD range, and even when the waveguide has only significant normal GVD across the entire range of frequencies. The dispersion of nonlinearity required for this effect can be achieved in subwavelength geometries where degree of light overlap with a nonlinear material strongly varies with wavelength. We also demonstrate, that a simple phenomenological model qualitatively reproducing this effect is the NLS equation with the intensity dependent GVD coefficient.

We consider a waveguide defined by the linear dielectric permittivity ε and nonlinear Kerr susceptibility $\chi^{(3)}$, both are functions of transverse coordinates $\vec{r}_\perp = (x,y)$, while the structure is homogeneous along the propagation direction z. The total field is sought as the sum of the pump, signal, and idler: $\vec{\mathscr{E}}(\vec{r},t) = \sum_{n=p,s,i} \mathbf{E}(\vec{r},\omega_n) e^{-i\omega_n t} + c.c.$. Each component is described in terms of the slowly varying amplitude $A_n(z)$ of the corresponding linear mode: $\mathbf{E}(\vec{r},\omega_n) = I_n^{-1/2} A_n(z) \mathbf{e}_n(\vec{r}_\perp) e^{i\beta_n z}$, where $I_n = \int\int_{-\infty}^{+\infty} (\mathbf{e}_n \times \mathbf{h}_n^* + \mathbf{e}_n^* \times \mathbf{h}_n)\, \hat{e}_z dxdy$, and $\hat{e}_z$ is the unit vector

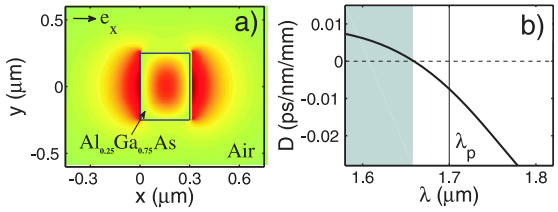

Fig. 1. Guided mode of $Al_{0.25}Ga_{0.75}As$ waveguide suspended in air: a) profile of the dominant electric field component (e_x) at $\lambda_p = 1.7\mu m$ for 500nm×300nm. Waveguide is indicated by solid lines; (b) calculated GVD, $D = -2\pi c\beta_2/\lambda^2$, white area indicates the range of normal GVD.

along z. $\mathbf{e}_n(\vec{r}_\perp)$ and $\mathbf{h}_n(\vec{r}_\perp)$ are the electric and magnetic field profiles of the linear mode, β_n is the corresponding propagation constant. The normalization is such that the power carried by the field n is given by $P_n = |A_n|^2$.

Displacement vector $\vec{\mathscr{D}}(\vec{r},t) = \sum_{n=p,s,i}\mathbf{D}(\vec{r},\omega_n)e^{-i\omega_n t} + c.c.$ is assumed to have the form: $\mathbf{D}(\omega_n) = \varepsilon_0\varepsilon(\omega_n)\mathbf{E}(\omega_n) + \varepsilon_0\chi^{(3)}(-\omega_n;\omega_k,-\omega_l,\omega_m)\vdots\mathbf{E}(\omega_k)\mathbf{E}^*(\omega_l)\mathbf{E}(\omega_m)$, where the third-order susceptibility tensor is given by $\chi^{(3)}_{iprs}(-\omega_n;\omega_k,-\omega_l,\omega_m) = \chi_{nklm}\left[\rho\left(\delta_{ip}\delta_{rs}+\delta_{ir}\delta_{ps}+\delta_{is}\delta_{pr}\right)/3+(1-\rho)\delta_{iprs}\right]$ [3], ρ is the nonlinear anisotropy parameter ($\rho = 1$ in the isotropic approximation). Using an approach identical to the one developed in [3, 8] we derive the following system of equations for the amplitudes of interacting waves:

$$i\partial_z A_n = -\sum_{k,l,m}\gamma_{nklm}e^{i(\beta_k+\beta_m-\beta_l-\beta_n)z}A_kA_l^*A_m\,, \tag{1}$$

$$\gamma_{nklm} = \frac{\varepsilon_0\omega_n}{\sqrt{I_nI_kI_lI_m}}\int\int_{-\infty}^{+\infty}\chi_{nklm}\zeta_{nklm}(\vec{r}_\perp)dxdy\,, \tag{2}$$

$$\zeta_{nklm} = \rho\left[(\mathbf{e}_n^*\mathbf{e}_m)(\mathbf{e}_k\mathbf{e}_l^*)+(\mathbf{e}_n^*\mathbf{e}_k)(\mathbf{e}_m\mathbf{e}_l^*)+(\mathbf{e}_n^*\mathbf{e}_l^*)(\mathbf{e}_k\mathbf{e}_m)\right]+3(1-\rho)\sum_{i=x,y,z}e_{ni}^*e_{ki}e_{li}^*e_{mi}\,. \tag{3}$$

For small signal and idler fields Eqs. (1) are reduced to

$$i\partial_z A_p = -\gamma_p|A_p|^2A_p\,, \tag{4}$$

$$i\partial_z A_s = -2\gamma_{sp}|A_p|^2A_s - \gamma_{4s}A_p^2A_i^*e^{i\delta\beta z}\,, \tag{5}$$

$$i\partial_z A_i = -2\gamma_{ip}|A_p|^2A_i - \gamma_{4i}A_p^2A_s^*e^{i\delta\beta z}\,, \tag{6}$$

with five different nonlinear coefficients: $\gamma_p \equiv \gamma_{pppp}$, $\gamma_{sp} \equiv \gamma_{spps}$, $\gamma_{ip} \equiv \gamma_{ippi}$, $\gamma_{4s} \equiv \gamma_{spip}$, $\gamma_{4i} \equiv \gamma_{ipsp}$. For $A_p(z) = \sqrt{P}e^{i\kappa_p z}$ with $\kappa_p = \gamma_p P$ and $A_s \sim e^{i\kappa_s z+gz+iqz}$, $A_i \sim e^{i\kappa_i z+gz+iqz}$, $\kappa_s = 2\gamma_{sp}P$, $\kappa_i = 2\gamma_{ip}P$ we find the MI gain g is given by:

$$g = \frac{1}{2}\mathrm{Re}\sqrt{(4\Gamma_+P-\delta\beta)(\delta\beta-4\Gamma_-P)}, \qquad \Gamma_\pm = \left(\gamma_{sp}+\gamma_{ip}-\gamma_p\pm\sqrt{\gamma_{4s}\gamma_{4i}}\right)/2. \tag{7}$$

The condition $g > 0$ is expressed as:

$$4\Gamma_-P < \delta\beta < 4\Gamma_+P\,. \tag{8}$$

By taking $\gamma_{sp} = \gamma_{ip} = \gamma_{4s} = \gamma_{4i} = \gamma$, we obtain $\Gamma_- = 0$ and $\Gamma_+ = \gamma$, and the routine condition $\delta\beta > 0$ is restored [12]. However, for $\Gamma_- < 0$ MI also exists if $\delta\beta < 0$, providing $P > P_{th} = |\delta\beta|/(4|\Gamma_-|)$. This is our central observation, various aspects of which are discussed below.

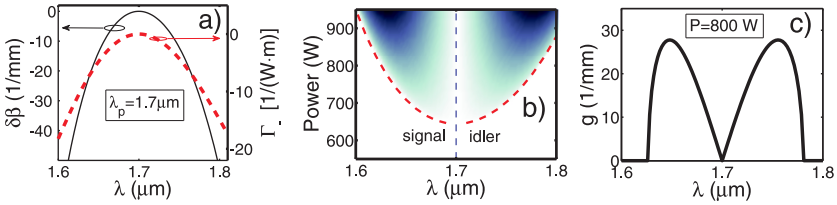

Fig. 2. MI in $Al_{0.25}Ga_{0.75}As$ waveguide: (a) $\delta\beta$ and Γ_- at $\lambda_p = 2\pi c/\omega_p = 1.7\mu m$ as functions of the signal/idler wavelengths. $n_2 = 1.5\cdot 10^{-17}\mathrm{m}^2/\mathrm{W}$, $D = -0.07 ps/nm/mm$; (b) gain as function of pump power and signal/idler wavelengths, $g > 0$ within shaded areas with darker colours corresponding to larger values of g. Dashed lines show the threshold power $P_{th} = \delta\beta/(4\Gamma_-)$; (c) gain as function of signal/idler wavelength for $P = 800W$.

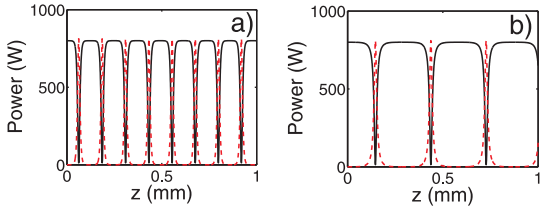

Fig. 3. Dynamics of the pump and signal waves for $\delta\beta > 0$ (a) and $\delta\beta < 0$ (b). Initial conditions: $P(z=0) = 800\mathrm{W}$, $P_s(z=0) = 0.8\mathrm{mW}$, $P_i(z=0) = 0$, $\lambda_p = 1.6\mu\mathrm{m}$, $\lambda_s = 1.55\mu\mathrm{m}$ (a), $\lambda_p = 1.7\mu\mathrm{m}$, $\lambda_s = 1.65\mu\mathrm{m}$ (b). Solid/dashed line corresponds to pump/signal.

Dispersion of nonlinearity is defined by three distinct contributions. First, is the material dispersion of the $\chi^{(3)}$ tensor; second, is the geometrical dispersion induced by dependencies of the modal profiles and of the overlap integrals on values of $\omega_{p,s,i}$; third, is that each γ_{nklm} is trivially proportional to ω_n. The latter factor acting on its own makes $\Gamma_- \sim \omega_p - \sqrt{\omega_p^2 - (\omega_p - \omega_s)^2} > 0$ and hence can not create MI gain with negative $\delta\beta$. Thus to achieve $\Gamma_- < 0$, one has to rely on material and geometrical contributions to the dispersion of nonlinearity. The material dispersion is usually weak and also poorly characterized in terms of its variations with multiple frequencies. Contrary, geometrical dispersion is expected to be strong and also controllable with the waveguide geometry and choice of the operating wavelength. Below we illustrate possibility of MI with $\delta\beta < 0$ in some ordinary waveguide geometries. Hereafter we take $\chi = (4/3)\varepsilon_0\varepsilon c n_2$, where n_2 is the constant Kerr coefficient and $\varepsilon = \varepsilon(\omega_p)$. The geometrical dispersion is accounted for by computing guided modes at the required frequencies with the help of the Comsol's Maxwell solver.

As our first example we consider a suspended $Al_{0.25}Ga_{0.75}As$ waveguide with the geometry and profile of one of the guided modes (dominant electric field component is oriented horizontally) shown in Fig. 1(a). The GVD of this mode is normal for $\lambda > 1.66\mu m$, see white area in Fig. 1(b). The full line in Fig. 2(a) shows the plot of $\delta\beta$ as function of the signal and idler wavelengths for $\lambda_p = 1.7\mu\mathrm{m}$. One can see that $\delta\beta$ is negative everywhere. Hence MI can be provided only through the mechanism related to the dispersion of nonlinearity and is possible only if $\Gamma_- < 0$. We have found that $\Gamma_- < 0$ in the broad range of the signal and idler frequencies, see the dashed line in Fig. 2(a), while Γ_+ is always positive. Thus, by increasing the pump power P, one can always satisfy the MI condition (8). The calculated gain together with the threshold pump power $P_{th}(\lambda_p)$ and typical MI gain profile are shown in Figs. 2(b) and (c), re-

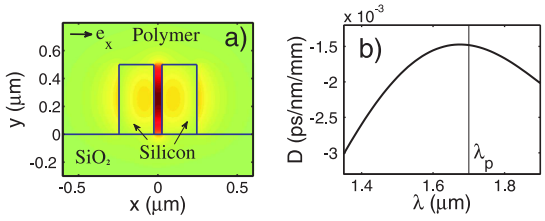

Fig. 4. Fundamental mode of the silicon-polymer slot waveguide: a) profile of the dominant electric field component (e_x) at $\lambda_p = 1.7\mu m$ for 500nm×220nm silicon waveguides, wall-to-wall separation 50nm, silica glass substrate and nonlinear polymer cladding. Geometry is indicated by solid lines; (b) calculated GVD.

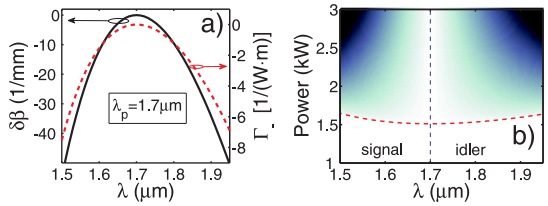

Fig. 5. The same as Figs. 2(a) and (b) but for the slot geometry, $\lambda_p = 1.7\mu$m ($D = -0.0015$), $n_{2,Polymer} = 16.9 \cdot 10^{-18} m^2/W$, $n_{2,Silicon} = 4 \cdot 10^{-18} m^2/W$, $n_{2,SiO_2} = 2.5 \cdot 10^{-20} m^2/W$.

spectively. For $P = 800$W, the maximum gain is achieved for $\lambda_s \approx 1.65\mu$m ($\lambda_i \approx 1.75\mu$m), and the characteristic MI length is $L_{MI} = 1/g \sim 0.03$mm. Assuming the excitation with picosecond pulses, $T_0 = 1$ps, we estimate the dispersion length, $L_D = T_0^2/|\beta_2| \sim 100$mm, and the walk-off length between the signal and idler, $L_w = T_0/|1/v_{gs} - 1/v_{gi}| \sim 1mm$, $v_{gs,gi} = 1/\partial_\omega \beta(\omega_{s,i})$ to be much longer than the MI length. This justifies our CW based approach to analyze MI, Eqs. (4-6). In Fig. 3 we illustrate the MI development along the waveguide length for the cases of $\delta\beta > 0$ ($\lambda_p = 1.6\mu$m) and $\delta\beta < 0$ ($\lambda_p = 1.7\mu$m). The results were obtained by numerical integration of Eqs. (1) for the case of three waves. During evolution, the energy from the pump is almost entirely transferred to the signal and idler, and then back to the pump again, the whole process repeats periodically with propagation distance. Such recurrence is typical e.g. for MI processes in optical fibres and is known to persist even with the full account of higher order harmonics [13]. Studies of possible modifications of the recurrence process due to the dispersion of nonlinearity in subwavelength structures are beyond the scope of present work.

To qualitatively estimate the impact of material dispersion of $\chi^{(3)}$, we also calculated $P_{th}(\lambda)$ by using $\chi_{nklm} = (4/3)\varepsilon_0 \varepsilon(\bar{\omega}_{nklm}) c n_2$, where $\bar{\omega} = (\omega_n + \omega_k + \omega_l + \omega_m)/4$. This gave only negligible deviations from the results shown in Fig. 2(b), thus confirming the dominant role of the geometrical dispersion of nonlinearity.

As our second example we consider a silicon-on-insulator dielectric slot waveguide with the nonlinear polymer cladding [14], see Fig. 4(a). Localization of the fundamental mode is sensitive to wavelength, and therefore the geometrical dispersion of nonlinearity is expected to be significant. GVD of a typical structure is shown in Fig. 4(b) and it is normal for any wavelength. Hence $\delta\beta < 0$, see Fig. 5(a), and without the dispersion of nonlinearity, no MI is expected for any pump wavelength. However, Γ_- has been found negative, see an example of the Γ_- dependence on the signal and idler wavelength for $\lambda_p = 1.7\mu$m shown in Fig. 5(a). Therefore, the MI condition (8) is satisfied for $P > P_{th}$, see Fig. 5(b). The ratio of the characteristic lengths (see Al-

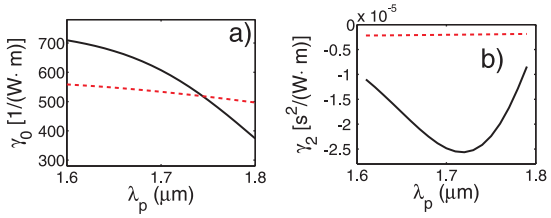

Fig. 6. Nonlinear parameters γ_0 (a) and γ_2 (b) for the waveguides as in Fig. 1 (solid lines) and Fig. 4 (dashed lines).

GaAs discussion) has also been found favorable for MI observation over typical sub-milimeter propagation distances, where walk-off due to GVD is negligible for picosecond pulses. Thus, while the frequency conversion in the optical processing experiment with a similar slot waveguide [14] has relied on the two frequency pumping (classical four wave mixing setup), our MI mechanism allows to obtain the necessary gain only with the single pump wave. Note also that two photon absorbtion and free carrier generation in AlGaAs are negligible for $\lambda \geq 1.5\mu$m. They are significant in silicon, but reduced in the slot geometry with the polymer cladding [14].

While the results presented above demonstrate the existence of MI induced by the dispersion of nonlinearity, they provide us with little intuition on why and where such behavior can be expected. Indeed, all the information needed to analyze MI condition in Eq. (8) is hidden inside the complex overlap integrals determining the values of γ_{nklm}. To formulate a more transparent qualitative approach to the problem, we introduce a generalized NLS equation where all the dispersion coefficients include nonlinear contributions $i\partial_z A = -\sum_{n=0}^{N} \frac{i^n}{n!}(\beta_n + \gamma_n|A|^2)\partial_t^n A$. Monochromatic solution of this equation is given by $A = ae^{i\kappa z - i\delta t}$, where $\kappa = \sum_n(\beta_n + \gamma_n|a|^2)\delta^n/n!$ and $\delta = \omega - \omega_p$. Thus the linear propagation constant is $\beta = \sum_{n=0}\beta_n\delta^n/n!$, while the frequency dependence of the nonlinear waveguide parameter γ is given by $\gamma = \sum_{n=0}\gamma_n\delta^n/n!$. Through the appropriate choice of the phase shift and of the reference velocity one can always fix $\beta_0 = \beta_1 = 0$. The minimal model capturing the nonlinearity induced MI is then

$$i\partial_z A = -i\gamma_1|A|^2\partial_t A + \frac{1}{2}(\beta_2 + \gamma_2|A|^2)\partial_t^2 A - \gamma_0|A|^2 A. \tag{9}$$

Expanding A as the sum for the pump, signal and idler waves we find $\gamma_{4s} = \gamma_{4i} = \gamma_0$ (note, that in the modal expansion $\gamma_{4s} \neq \gamma_{4i} \neq \gamma_p$), $\gamma_{sp} = \gamma_0 - \gamma_1\delta + \gamma_2\delta^2$, and $\gamma_{ip} = \gamma_0 + \gamma_1\delta + \gamma_2\delta^2$. Using our previous notations it is clear that $\gamma_0 = \gamma_p$. Thus the MI condition for $\delta\beta < 0$ transforms into: $\Gamma_- = \gamma_2\delta^2 < 0$. For the relatively small δ we have $\gamma_n = \partial_\omega^n\gamma$. γ and its second derivative $\partial_\omega^2\gamma$ for the waveguides considered above are plotted in Figs. 6(a) and (b), respectively. These plots show that $\partial_\omega^2\gamma < 0$ and thus confirm that the calculation of the several overlap integrals and much simpler differentiation of γ yield the same prediction about existence of MI induced by the dispersion of nonlinearity.

In summary: Using modal expansion we have demonstrated that the confinement induced dispersion of nonlinearity creates conditions for observation of MI in subwavelength AlGaAs and silicon waveguides with large normal GVDs. We calculated the pump power thresholds required for this type of MI to be around 1kW and presented a generalization of the NLS equation accounting for this effect. To reduce the threshold power to levels more favorable for applications, further understanding of the relevant physics and design work are necessary.

This work is supported by the UK EPSRC project EP/G044163. We acknowledge useful comments from M. Sorel on properties of AlGaAs waveguides.